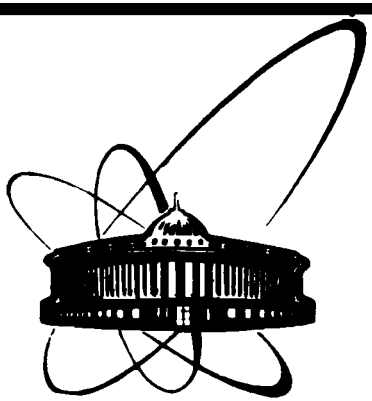

Объединенный
институт
ядерных
исследований
дубна

E2-89-666

M.G.Dolidze*, G.I.Lykasov

FRAGMENTATION OF DEUTERONS ON NUCLEONS IN THE INFINITE MOMENTUM FRAME

Submitted to "Zeitschrift für Physik A"

* TSU, Tbilisi, GSSR

1989

INTRODUCTION

The investigation of the interaction of fast deuterons with nucleons and nuclei can give new information about relativistic properties of the deuteron and the interaction dynamics of the deuteron at small distances especially in the fragmentation region. The decay vertex of the deuteron into two nucleons is related with its wave function which can be the solution of the Bethe-Salpeter equation for the bound state in the general relativistic case. But there is still no exact simple solution of this equation. Therefore we must resort to different approximations. It is better to use the infinite momentum frame (IMF) in which the notion of the deuteron wave function (w.f.d.) of dynamics of the light cone may be introduced [1-4], its square having the usual probable interpretation. The w.f.d. depending on the light cone variable x and the transverse momentum $\vec{K}_t$ of the intradeuteron nucleon is related to the nonrelativistic w.f.d. depending on the relativistic invariant variable [5-8].

The formalism [1-8], where the notion of WFD is introduced in IMF is further developed in this paper. Here the role of the nonspectator graphs is analysed in detail. The special attention is given to the analysis of the polarisation characteristics, in particular, deuteron tensor polarisation T_{20}. That is very interesting due to the experiments carried out now [9,10].

I. THE AMPLITUDE OF THE PROCESS $dN \to PX$

As mentioned above, it is better to consider the processes of type $dN \to PX$ in the IMF. As known, along with the covariant formalism the noncovariant one can be used, where each Feynman graph of the n-order is equivalent to $n!$ time-ordered graphs of the old perturbative theory (OPTh), a large part of them vanishe in IMF. In particular, of all graphs of the first and second order in hadron-nucleons (h-N) interactions in the process $dN \to PX$ only the graphs of Fig. 1 (a-e) type do not vanish in OPTh. As shown in refs [11-13] the graphs of Fig. 1 b [11] and 1 c [12] give great contributions to the proton

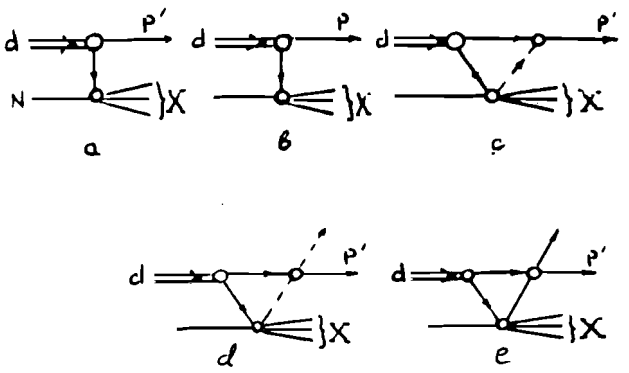

Fig. 1. Graphs corresponding to the process $dP \to PX$.

spectrum and the graphs of Fig. 1 d [12] and 1 e [13] give small contribution in some kinematic region. The four-momenta of the fast deuteron P_d and of its nucleons K_1, K_2 are represented in the IMF in the following form [13]:

$$P_d\left(P + \frac{M_d^2}{2P}, Q_t, P\right)$$
$$K_1\left(xP + \frac{m^2+\vec{K}_t^2}{2xP}, K_t, xP\right) \qquad (1)$$
$$K_2\left((1-x)P + \frac{m^2+\vec{K}_t^2}{2(1-x)P}, -\vec{K}_t, xP\right),$$

where P is the momentum of the projectile deuteron which must be infinitely large in principle; x is the longitudinal momentum fraction of the nucleon in the deuteron K_t is the transverse momentum of the intradeuteron nucleon. At the infinite P x is equivalent to the light cone variable.

According to ref. [6,8], as mentioned above the notion of the w.f.d. can be introduced in the IMF which depends on x and K_t $\Psi(x,\vec{K}_t)$. This w.f.d. can be related, according to refs [6,8] to the nonrelativistic w.f.d. $\Phi_{n.r.}$ depending on the relativistic invariant variable ε^2:

$$\Psi(x,K_t) = \left(\frac{m^2+\vec{K}_t^2}{4x(1-x)}\right)^{1/4} \Phi_{n.r.}(\varepsilon^2), \qquad (2)$$

where $\varepsilon^2 = \frac{m^2+\vec{K}_t^2}{4x(1-x)} - m^2$.

Here $\Psi(x,K_t)$ is normalized in the following way [6]:

$$\int_0^1 \frac{dx}{x(1-x)} \int d^2\vec{K}_t \, |\Psi(x,K_t)|^2 .$$

We shall now represent the general expression for the amplitude of the process $dN \to PX$ corresponding to the graphs of figs 1 (a-e) in the following form:

$$F = C \sum_{i=1}^{5} F_d^{(i)}, \qquad (3)$$

where the following notion is introduced: $C=(2(2\pi)^3)^{1/2}$ is the normalization coefficient /13/; $F_d^{(i)}$ are the amplitude parts corresponding to the graphs of figs 1 (a-e):

$$F_d^{(1)} = f_{1,NN}\,\Psi(x_1,\vec{K}_t);\quad F_d^{(2)} = f_{2,NN}\,\Psi(x_2,-\vec{K}_t), \qquad (4)$$

where $f_{1,NN}$, $f_{2,NN}$ are the amplitudes of N-N interactions corresponding to the lower vertices of figs 1a and 1b graphs; x_1, $\vec{K}_t$ correspond to the proton emitted from the upper vertex of fig. 1 a, i.e. to the spectator proton; x_2, $-\vec{K}_t$ correspond to the proton emitted from the lower vertex of fig. 1b, i.e. to the nonspectator one.

As mentioned above, the graphs of fig. 1 (c-e) can be calculated in the same way as in the OPTh but the non-relativistic w.f.d. is replaced by $\Psi(x,\vec{K}_t)$. The general expression for the graphs of figs 1(c-e) can be written in the following form:

$$F_d^{(3\text{-}5)} = -\frac{qP}{(2\pi)^3}\int \frac{\Gamma_N^{(1)}\Gamma_N^{(2)}dx}{2\sqrt{E(\vec{K}_1)E(\vec{K}_2)E(q)}}\int \Psi(x,\vec{K}_t)G(x,\vec{K}_t)\,d^2\vec{K}_t, \qquad (5)$$

where the following notion is introduced; $\Gamma_N^{(1)}$, $\Gamma_N^{(2)}$ are the lower and upper vertices of the h-N interactions in the graphs of figs 1 (c-e) respectively; $G(x,\vec{K}_t)=[E_d - E(\vec{K}_1) + m - E(\vec{q}) - E_X + i\varepsilon]^{-1}$ is the two-particle free Green function, in terms of the variable x and K_t it has the following form:

$$G(x,K_t) = \left[E' - P' - \frac{m^2+\vec{K}_t^2}{2xP} - \frac{m_R^2+\vec{K}_t^2}{2(P'-xP)} + i\varepsilon\right]^{-1}, \qquad (6)$$

where m, m_R are the masses of the nucleon, and the intermediate particle respectively. For all graphs in figs. 1(c-e) $\Gamma_N^{(1)}$ corresponds to the process $hN \to RX$, where R is the intermediate particle (the meson in figs 1 c,d and the nucleon in fig. 1 e). The $\Gamma_N^{(2)}$ vertex corresponds to the absorption of the virtual meson by nucleon in fig. 1 c, but if the meson is a pseudoscalar one,

then $\Gamma_N^{(2)} = \vec{\sigma}_N \cdot \vec{\tau}$, where $\vec{\tau} = \frac{\vec{P}-\vec{K}_t}{2m} - \frac{E'-E(\vec{K}_t)}{8m^2}(\vec{P}'+\vec{K}_t)$.

For the graphs of fig. 1 d and 1 e $\Gamma_N^{(2)}$ corresponds to the processes $RN \to PX$.

The calculating procedure of type (5) expression is sufficiently simplified if the proton in the reaction $dN \to PX$ is emitted either forward or at a small angle. Then the dependence of $G(x,\vec{K}_t)$, $\Gamma_N^{(1)}$ and $\Gamma_N^{(2)}$ on $\vec{K}_t$ can be neglected but the integral over $d^2\vec{K}_t$ is easily calculated if we use relation (2) and a realistic function, for example of type /14/ is taken as $\Phi_{n.r.}(\alpha^2)$. Then one can factor vertices $\Gamma_N^{(1)}$ and $\Gamma_N^{(2)}$ outside the integral sign at some x_0 corresponding to the mean value of the intradeuteron nucleon momentum, because $\Psi(x,\vec{K}_t)$ integrated over $d^2\vec{K}_t$ is the sharply decreasing function with x. After those simplifications the type (5) expressions for $F_d^{(3\text{-}5)}$ are easily calculated.

We shall now analyse the special type of the deuteron fragmentation processes on the nucleon when the proton is emitted forward or backward in the deuteron rest system. Those processes of the cumulative proton production are very interesting, as mentioned above. In ref. /12/ it is shown, that the contribution of the fig. 1 d graph can be noticeable in some kinematic region of the cumulative protons but about three times smaller than that of fig. 1 c. The contribution of the graphs of fig. 1 e type can be neglected in comparison with other graphs as the calculation results showed in ref. /13/. Then we shall keep the main contributions, i.e. the graphs of figs 1 (a-c) type. In the graph of fig. 1 c type both the pseudoscalar and vector meson can be the intermediate particle. If the energies of the projectile deuteron are not very large, for example $E_d \approx 10 \div 20$ (GeV), then the production of the vector mesons in the lower vertex of the fig. 1 c graph is very small in comparison with the pseudoscalar meson production as the experimental data show /15,16/. Therefore we can neglect the contribution of the fig. 1 c type graph with the absorption of the virtual vector mesons by nucleon and we shall keep the graphs of fig. 1 c with the pseudoscalar mesons in the intermediate state. Then the vertex $\Gamma_N^{(1)}$ in the graph of fig. 1 c can be related to the amplitude of the real meson production in the N-N interaction multiplied by the formfactor F_π that takes into account the off-shell effects of the virtual π-meson /12/. Taking into account all mentioned above, the amplitude of the investigated process is written in the following form:

$$F_d = f_{1,NN}\Psi(\alpha_1^2) + f_{2,NN}\Psi(\alpha_2^2) - F_d^{(3)}, \qquad (7)$$

where:

$$F_d^{(3)} = \vec{\sigma}_3\,\vec{\tau}^0 g\sqrt{m}\,P f_{N\to\pi}(x_0 P Q^2(x_0))\times$$

$$\times\{I_1 - \frac{1}{8}[3(\vec{\sigma}_p\vec{K}^0)(\vec{\sigma}_n\vec{K}^0) - \vec{\sigma}_p\vec{\sigma}_n]\,I_2\},$$

$$I_1 = \sum_{i=1}^{S} A_i \int_0^1 dx\,\frac{G(x)F_\pi(Q^2)(x(1-x))^{3/4}}{\sqrt{E(\vec{K}_1)E(\vec{K}_2)E_\pi(\vec{q})}}|\vec{\tau}|\exp(-\alpha_i m^2\,\frac{1-4x(1-x)}{4x(1-x)},$$

$$I_2 = \sum_{i=1}^{S} \frac{B_i}{\beta_i}\int_0^1 dx\,\frac{G(x)F_\pi(Q^2)(x(1-x))^{3/4}}{\sqrt{E(\vec{K}_1)E(\vec{K}_2)E_\pi(\vec{q})}}|\vec{\tau}|[m^2(1-4x(1-x)) + \frac{4x(1-x)}{\beta_i}]\exp$$

$$\left\{-\beta_i m^2\,\frac{1-4x(1-x)}{4x(1-x)}\right\},$$

$Q^2=(E'-E(\vec{K}_1))^2-\vec{q}^2$; $\vec{q}=\vec{P}'-\vec{K}_1$; $\vec{\tau}^0=\vec{\tau}/|\vec{\tau}|$, $\vec{\sigma}_N$ are Pauli's matrices corresponding to the nucleon, which absorbs the virtual π-meson (see fig. 1 c); $A_i, \alpha_i, B_i, \beta_i$ are the parameters of the w.f.d. /14/, the form of $\Phi_{n.r.}$ (2) is presented in the Appendix.

Having obtained expression (6) for the amplitude F_d of the process $dN \to PX$, we can now calculate the inclusive proton spectra, polarisation characteristics and analyse them in detail.

II. INCLUSIVE PROTON SPECTRA AND POLARIZATION PHENOMENA

The spin structure of the elastic N-N scattering amplitude can apparently be neglected at high energies as the experimental data indicate /17,18/. If we suppose that it is true for inelastic N-N collisions, then, according to (6), we can calculate both the inclusive spectrum of protons and the polarization characteristics. Then interference between the graphs of figs 1 a,b and 1 c vanishes. The general expression for the inclusive proton spectrum of the investigated reaction is written in the following form:

$$\rho_{dN} \equiv E'\frac{d\sigma_{dN}}{d^3\vec{P}'} = \frac{C^2(2\pi)^4}{4\lambda^{1/2}(S_{pd},m^2,M_d^2)}\times \qquad (8)$$

$$\times\int\delta^4(P_{in}-P_f)\,Sp(\rho_0 F_d^+ F_d)\,d\Gamma,$$

where: $\rho_0=\frac{1}{6}P_T$; $P_T=\frac{3+\vec{\sigma}_p\vec{\sigma}_n}{4}$ is the projection operator of the basic triplet state; $\lambda^{1/2}(x,y,z)=(x-y-z)^2-4yz)^{1/2}$;

$d\Gamma=\prod_{i=2}^{n}\frac{d^3P_i}{2(2\pi)^3E_i}$ is the phase volume of n-1 particles; $P_2, \ldots, P_4$; $E_2, \ldots, E_n$ are three-momenta and energies of final particles produced in lower vertices of figs 1 (a-e) graphs. It is better to write expression (8) in the following form:

$$\rho_{dN} = \rho_{dN}^{(1)} + \rho_{dN}^{(2)} + \rho_{dN}^{(3)}, \qquad (9)$$

where $\rho_{dN}^{(1)} = \frac{I_{NN}}{I_{dN}}\,\frac{|\Psi(x)|^2}{2(1-x)}\,\sigma_{NN}^{tot}$

$$\rho_{dN}^{(3)} = R\,|I|^2\left\{\rho_{pp\to\pi^+x} + \rho_{pp\to\pi^0x} + 2\sqrt{\rho_{pp\to\pi^+x}\,\rho_{pn\to\pi^0x}}\right\},$$

$R=\frac{I_{NN}}{I_{Nd}}$; I_{NN}, I_{dN} are the invariant fluxes in the N-N and d-N reactions respectively; $\rho_{pp\to\pi^+x}$, $\rho_{pn\to\pi^0x}$ are the invariant inclusive spectra of π^+ - and π^0-mesons in the reactions $PP\to\pi^+X$ and $Pn\to\pi^0X$ respectively, σ_{NN}^{tot} is the total cross section of N-N scattering, $\rho_{dN}^{(2)}$ is the contribution of the fig. 1 b graph and the interference between figs 1 a and 1 b to the total spectrum ρ_{dN}, its expression is presented in the Appendix.

We shall now consider a very interesting polarization characteristic, the tensor polarization component T_{20}, recently measured in the stripping-type reaction $dA \to PX$, $dP \to PX$ /9, 10/. The general expression for T_{20} in the discussed reaction is written in the following form:

$$T_{20} = \frac{\int Sp(\rho_0 F_d^+ \Omega_{20} F_d)\,d\Gamma}{\int Sp(\rho_0 F_d^+ F_d)\,d\Gamma}, \qquad (10)$$

where $\Omega_{20}=\frac{1}{\sqrt{2}}\left\{\frac{3}{2}(1+\sigma_{pz}\sigma_{nz})-2\right\}$ is the spintensor operator corresponding to the deuteron polarization component T_{20}; σ_{pz}, σ_{nz} are the Z-components of Pauli's matrices corresponding to the proton and to the neutron.

The spin structure of the relativistic w.f.d. Ψ is equivalent to the spin structure of the nonrelativistic w.f.d. $\Phi_{n.r.}$ /14/, as shown in ref. /6/, in the case when the proton is emitted forward in the reaction $dN \to PX$

$$\Psi = \Psi_0 - \frac{1}{\sqrt{8}} S_{pn} \Psi_2 , \qquad (11)$$

where $S_{pn} = 3(\vec{\sigma}_p \vec{K}^0)(\vec{\sigma}_n \vec{K}^0) - \vec{\sigma}_n \vec{\sigma}_p$, $\vec{K}^0$ is the unit vector of the relative momentum of the proton and the neutron. Then assuming as mentioned above, the nonspin structure of the N-N interaction amplitude and substituting (10) into (6) and (6) into (9), we obtain the final expression for T_{20}:

$$T_{20} = -\frac{1}{\sqrt{2}} \frac{2\sqrt{2}\Psi_0\Psi_2 + \Psi_2^2 + \tilde{R}_2 + R_1(2\sqrt{2}\,\mathrm{Re}\, I_1^* I_2) + |I_2|^2)\,\rho_{N\pi}/\sigma_{NN}^{tot}}{\Psi_0^2 + \Psi_2^2 + R_2 + R_1(|I_1|^2 + |I_2|^2)\,\rho_{N\pi}/\sigma_{NN}^{tot}} , \qquad (12)$$

where the following notion is introduced: $\tilde{R}_2$, R_2 are the expressions corresponding to the contributions of the fig. 1 b graph and the interference between fig. 1 a and 1 b respectively, they are presented in the Appendix; $\rho_{N\pi} = \rho_{pp\to\pi^+X} + \rho_{pn\to\pi^0X} + \rho^{int}$;

$$\rho^{int} \cong 2\sqrt{\rho_{pp\to\pi^+X}\ \rho_{pn\to\pi^0X}} \ ; \quad R_1 = R\,\frac{I_{Nd}}{I_{NN}}\,2(1-x) .$$

It is seen from expression (11) that (10) turns into a usual formula for T_{20} in the spectator mechanism, i.e. when, only the pole graph of fig. 1 a is taken into account.

$$T_{20} = -\frac{1}{\sqrt{2}} \frac{2\sqrt{2}\,\Psi_0(\text{æ}^2)\Psi_2(\text{æ}^2) + \Psi_2^2(\text{æ}^2)}{\Psi_0^2(\text{æ}^2) + \Psi_2^2(\text{æ}^2)} . \qquad (13)$$

We shall now return to the calculation results of the inclusive spectrum using (8) and of its separate contributions $\rho_{dN}^{(1)}$, $\rho_{dN}^{(2)}$, $\rho_{dN}^{(3)}$, the tensor polarisation T_{20}. Some details of the calculations (forms of spectra $\rho_{pN\to\pi^0X}$, of NN-interaction amplitudes, of the meson form factor F_π, etc.) are presented in the Appendix.

The calculation curves corresponding to the total proton spectrum ρ_{dN} and to the separate contributions of figs 1 (a-c) graphs and the experimental data /20/ are presented in fig. 2. It is seen that we cannot confine ourselves to the contribution of one spectator graph in the momentum region of protons scattered backward in the deuteron rest frame $0.15 \le q \le 0.45$, the interference between the

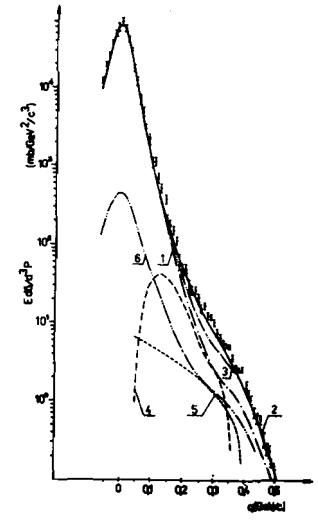

Fig. 2. Dependence of the inclusive proton spectrum in the reaction $dP \to PX$ on the final proton momentum in the deuteron rest frame:
Curves: 1 - contribution of the spectator graph of fig. 1 a to the spectrum; 2 - summed contribution of the graphs of figs 1 a-c to the spectrum; 3 - contribution of the figs 1 a-b graphs; 4 - contribution of the fig. 1 c type graphs; 5 - contribution of the figs 1 d graphs; ϕ - the experimental data at $E_d = 9$ (GeV).

graphs of figs 1 a and 1 b and especially the graph of fig. 1 c give noticeable contributions. Calculated curve 3 on fig. 2 corresponding to the proton spectrum ρ_{dN}, if the graphs of figs. 1 a-c type are taken into account rather satisfactorily agrees with the experimental data at $E_d \approx 9$ (GeV).

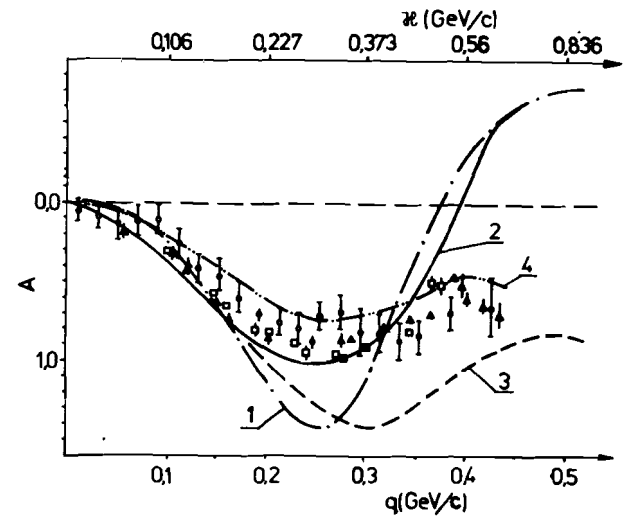

Fig. 3. Dependence of $A = \sqrt{2}\,T_{20}$ on the final proton momentum q in the deuteron rest frame and on the internal nucleon momentum in the deuteron æ;
Curves; 1 - contribution of the spectator mechanism, fig. 1a; 2 - contribution of figs 1 a-c graphs; 3 - calculation result from ref. /22/; 4 - T_{20} with the complex 6q-component in the deuteron included (see (14)); experimental data: ϕ - from ref. /10/, ϕ, ϕ - from ref. /9/.

The calculation results of the tensor polarisation component T_{20} and the experimental data [9,10] for the reaction $dA \to PX$, where A=H [9], Cu [9,10], Al [9], are presented in fig. 3. T_{20} weakly depends on the atomic number A and the energy of the initial deuteron as the experimental data show. Therefore our calculations of T_{20} for the process $dN \to PX$ can be compared with the available experimental data. It is seen from fig. 3 that the graphs of fig. 1c type give the noticeable contribution to T_{20} at $q \leq 0.4$ (GeV/c) or $\alpha \leq 0.55$ (GeV/c). In principle the discrepancy between curve 2 in fig. 3 and the experimental data at $q > 0.4$ (GeV/c) can be due to different causes: the neglect of the spin structure of the N-N interaction amplitudes the neglect of the figs 1 d-e graphs, which give at least small contributions to the inclusive proton spectrum. But we shall note that T_{20} is sufficiently sensitive to different relativisation methods of the deuteron structure. So in ref.[21,22] another method of the inclusion of relativistic effects is proposed, which differs from the method used in this paper. Curve 3 in fig. 3 is the calculation result of T_{20} taken from ref. [22] in the frame of the spectator mechanism. It is seen from the comparison of curves 1 and 3 in fig. 3 that the behaviour of T_{20} depends rather on the method of inclusion of the relativistic effects in the deuteron at $q \geq 0.4$ (GeV/c) or $\alpha \geq 0.55$ (GeV/c). For this reason in some papers [9] some addition to the deuteron wave function caused by the probable existence of the six-quark state is introduced. But it was necessary for the successful description of the experimental data on T_{20} in the spectator mechanism frame that it was complex at the phase $\varphi = 55^\circ$ [9], i.e. the w.f.d. is represented in the form:

$$\tilde{\Psi}(x) = (1-\omega)\Psi(x) + \omega\Delta(x)e^{i\varphi}, \qquad (14)$$

where ω is the probability of the existence of the non-nucleon component in the deuteron. If the graphs of figs. 1 a-c are taken into account, then, as the calculations have shown, the complex 6q-component will be necessary to describe the T_{20} experimental data at $q \geq 0.4$ (GeV/c) (see curve 4 in fig. 3). Here the 6q-state in the deuteron is taken into account according to ref. [23]. The curve 4 corresponding to the w.f.d. $\tilde{\Psi}(x)$ of the type (14) at $\varphi = 110^\circ$ is presented in fig. 3. This complexity contradicts the quantum-mechanical principles, because a bound state particularly that of the deuteron, is described by a real function. We think, therefore, that the discrepancy of calculated curve 2 with the T_{20} experimental

data at $q \geq 0.4$ (GeV/c) can't be a direct indication of the 6q-state existence in the deuteron.

Note that the contribution of this 6q-component to the inclusive spectrum of the investigated reaction is negligibly small at the initial energy of the deuteron $E_0 = 9$ GeV as it is shown in ref. [12].

CONCLUSION

The calculation results presented in figs 2,3 allow the following conclusions. It is just incorrect to use the spectator mechanism, i.e., fig. 1 a graph, for the analysis of the deuteron stripping type reaction. As is very clearly shown in fig. 2, it is necessary to take into account the nonspectator type graphs of fig. 1 b,c at $0.15 \leq q \leq 0.5$ (GeV/c). Therefore the measurement of the proton inclusive spectrum in the discussed reactions is not the direct measurement of the square of the WFD. The contribution of the fig. 1 b,c graphs can't be considered as a small correction to the fig. 1a graph at $q \geq 0.15$ (GeV/c). The inclusion of the fig. 1 b,c graphs allows a much better description of the T_{20} experimental data at $q \leq 0.4$ (GeV/c). The great discrepancy between calculated curve 2 in fig. 3 and the experimental data at large proton momenta, $q \geq 0.4$ (GeV/c) can be due different causes. As is mentioned above T_{20} can be sensitive to the relativistic deuteron structure. The comparison of curves 2 and 3 in fig. 3 allows the following conclusion. The reaction mechanism, i.e. the fig. 1 (a-c) graphs, must be taken into account more completely at small q, $q \leq 0.4$ (GeV/c) but the relativisation effects of the vertex of the deuteron decay into two nucleons are very important at larger q or $\alpha > 0.55$ (GeV/c). Different relativisation methods yield different T_{20} behaviour at $q > 0.4$ (GeV/c). Besides, the discrepancy between calculated curve 2 and T_{20} experimental data at $q > 0.4$ (GeV/c) can't be a direct indication of the 6q-state existence in the deuteron, because of the complexity of the 6q-addition to the w.f.d.

ACKNOWLEDGEMENTS

The authors would like to express their profound gratitude to V.V.Anisovich, V.V.Burov, L.G.Dachno, A.V.Efremov, V.A.Karmanov, A. .Kvinikhidze, L.A.Kondratyuk, L.N.Strunov, I.N.Sitnik, B.Tecoult, I.S.Shapiro for useful advises and discussions.

APPENDIX

The nonrelativistic w.f.d. $\Phi_{n.r.}(\varkappa^2)$ has the following form /14/:

$$\Phi_{n.r.}(\varkappa^2)=\left\{u(\varkappa^2)-\frac{1}{\sqrt{8}}\,\omega(\varkappa^2)S_{np}\right\}\chi\,, \qquad (A1)$$

where u , ω are S- and D-waves of the w.f.d.; χ is the spin triplet wave function $S_{np}=\left\{3(\vec{\sigma}_n\vec{K}^o)(\vec{\sigma}_p\vec{K}^o)-\vec{\sigma}_n\vec{\sigma}_p\right\}$; $\vec{K}^o$ is the unit vector of the relative momentum of the nucleons in the deuteron. According to ref. /14/ u,ω are represented in the following form:

$$u(\varkappa^2)=\sum_{i=1}^{5}A_i e^{-\alpha_i\varkappa^2}\,,\quad \omega(\varkappa^2)=\sum_{i=1}^{5}B_i e^{-\beta_i\varkappa^2}\,, \qquad (A2)$$

values A_i , α_i and B_i β_i are represented in ref. /14/.

The form of F_d is given by the expression of (7). It $f_{1,NN}$; $f_{2,NN}$; $f_{N\to\pi}$ do not depend on the spin of nucleons then the interference between the third and other terms in (7) vanishes during the calculation of the expression $Sp(\rho_0 F_d^+ F_d)$ entering into (8). Then we have:

$$Sp\left\{\rho_0 F_d^+ F_d\right\}=Sp\left\{\rho_0 F_d^{(1,2)+}F_d^{(1,2)}\right\}+Sp\left\{\rho_0 F_d^{(3)+}F_d^{(3)}\right\}, \qquad (A3)$$

where

$$F_d^{(1,2)}=f_{1,NN}\Psi(\varkappa_1^2)+f_{2,NN}\Psi(\varkappa_2^2)$$

$$Sp\left\{\rho_0 F_d^{(1,2)+}F_d^{(1,2)}\right\}=|f_{1,NN}|^2|\Psi(\varkappa_1^2)|^2+|f_{2,NN}|^2|\Psi(\varkappa_2^2)|+$$

$$+2Re\left\{f_{1,NN}^+ f_{2,NN}\right\}\left\{u(\varkappa_1^2)u(\varkappa_2^2)+\frac{3\vec{K}^o\vec{K}^{o\prime}-1}{2}\,\omega(\varkappa_1^2)\omega(\varkappa_2^2)\right\}.$$

The following method was used for the calculation of the contributions of the fig. 1 b graph and the interference between the graphs of figs 1 a and 1 b . It was assumed that in the lower vertex of figs 1 a and 1 b two particles are produced in the final state, one of them is the particle of some effective mass M_X then it was summarised over different M_X . The amplitudes of these binar processes

$f_{1,NN}$, $f_{2,NN}$ for a certain M_X were taken from ref. /24/. The expression for $\rho_{dN}^{(2)}$ at a fixed M_X has then the following form:

$$\rho_{dN}=\frac{C^2}{(2\pi)^4 16\lambda^{1/2}(S_{pd},m^2M_d^2)}\int_0^1\frac{|F|^2}{1-x_1}dx_1$$

$$|F|^2=|f_{2NN}|^2|\Psi(\varkappa_2^2)|+2Re(f_{1,NN}^+ f_{2,NN})\left\{u(\varkappa_1^2)u(\varkappa_2^2)+\right. \qquad (A4)$$

$$\left.+\frac{1}{2}(3K^oK^o-1)\omega(\varkappa_1^2)\omega(\varkappa_2^2)\right\}.$$

The second summand in (A4) is the interference between the graphs of figs 1 a and 1 b.

We shall present now the expression for R_2, $\tilde{R}_2$ entering into (12).

$$R_2=\rho_{dN}^{(2)}\frac{I_{Nd}}{I_{NN}}2(1-x)/\sigma_{NN}^{tot}$$

$$\tilde{R}_2=\frac{1}{\sqrt{2}\rho_{dN}}\int\left\{g_1|f_{1,NN}|^2+g_2|f_{2NN}|^2+g_3\,2Re(f_{1,NN}^+ f_{2NN})\right\}\frac{d\Gamma}{I_{Nd}}$$

$$g_1=2\sqrt{2}\,\Psi_0(\varkappa_1^2)\Psi_2(\varkappa_1^2)+\Psi_2^2(\varkappa_1^2)$$

$$g_2=[2\sqrt{2}\,\Psi(\varkappa_2^2)\Psi_2(\varkappa_2^2)+\Psi_2^2(\varkappa_2^2)]\frac{3\vec{K}_z^{o\prime}-1}{2}$$

$$g_3=\sqrt{2}\left[\Psi_0(\varkappa_2^2)\Psi_2(\varkappa_1^2)+\frac{3(K_z^{o\prime})-1}{2}\Psi_0(\varkappa_1^2)\Psi_2(\varkappa_2^2)+\Psi_2(\varkappa_2^2)\Psi_0(\varkappa_1^2)\frac{3(K_z^{o\prime})-1}{2}\right.$$

$$\vec{K}_z^{o\prime}=\vec{K}_0^o\vec{K}^{o\prime};\quad \vec{K}^o\parallel\vec{z}\,.$$

References

1. Brodsky Stanley J. et al. Phys.Rev., v. D8, p. 4574 (1973).
2. Kogut John B. and Soper Davison E. Phys.Rev., 1970, v. 1, p. 2901.
3. Chemtob M. Nucl.Phys., 1979, v. A314, p. 387.
4. Weinberg S. Phys.Rev., 1966, v. 150, p. 1313.

5. Frankfurt L.L., Strikman M.I. Phys.Rep., 1981, v. 76, p. 215.
6. Karmanov V.A. EPAN, 1988, v. 19, No 3, p. 525.
7. Garsevanishvili V.R. XIII Winter School of Theoretical Physics in Kappacz, 1976, v. 1, p. 313.
8. Kobushkin A.P., Vizireva L.J. IRP-81-108E; J.Phys.G: Nucl.Phys., 1982, v. 8, p. 893.
9. Perdrisat C.F. et al. Phys.Rev.Lett., 1987, v. 59, p. 596.
10. Ableev V.G. et al. JETP Lett., 1988, v. 47, p. 558.
11. Dakhno L.G., Nikonov V.A. Nucl.Phys.
12. Ignatenko M.A., Lykasov G.I. Jad.Fis., 1987, v. 46, p. 1080.
13. Dolidze M.G., Lykasov G.I. JINR, 1988, E2-88-133.
14. Reid R.V.Jr. Ann.of Phys., v. 50, p. 414 (1968).
15. Grassler H. et al. Nucl.Phys., B132, p. 1 (1978).
16. Akesson T. et al. Nucl.Phys., v. B203, No 1, p. 27 (1982).
17. Lapidus L.I. EPAN, v. 15, p. 493 (1984).
18. Ranft G., Ranft I. EPAN, v. 15, p. 555 (1984).
19. Bugg D.V. and Wilkin C. Phys.Lett., v. 152B, p. 37 (1985); v. 154B, p. 243 (1985).
20. Ableev V.G. et al. JETP Lett., v. 45, p. 596 (1987).
21. Braun M.A. Jad.Fiz., v. 42, p. 816 (1985).
22. Braun M.A., Tokarev M.V. Proc.of Symposium Nucleon-Nucleon and Hadron-Nucleus Interactions at Intermediate Energies. Leningrad, 1986, p. 311.
23. Efremov A.V. et al. Jad.Fiz., v. 47, p. 1364 (1988).
24. Azhgirey L.S., Razin S.V., Yudin N.P. - Jad.Fis., v. 46, p. 1657 (1987).
Azhgirey L.S. et al. JINR P2-87-417, Dubna, 1987.

Received by Publishing Department
on September 21, 1989.

Долидзе М.Г., Лыкасов Г.И. E2-89-666

Фрагментация дейтронов на нуклонах
в системе бесконечного импульса

Развит метод анализа взаимодействия быстрых дейтронов с нуклонами. При этом учитываются как релятивистские эффекты в дейтроне, так и механизм их взаимодействия. На примере процессов типа фрагментации дейтронов на нуклонах исследуются инклюзивные спектры протонов и поляризационные характеристики. Показывается сильная чувствительность тензорной компоненты поляризации дейтрона T_{20} как к механизму реакции, так и к релятивистской структуре дейтрона. Обсуждается возможное проявление 6q-состояния в дейтроне в таких реакциях.

Работа выполнена в Лаборатории ядерных проблем ОИЯИ.

Препринт Объединенного института ядерных исследований. Дубна 1989

Dolidze M.G., Lykasov G.I. E2-89-666

Fragmentation of Deuterons on Nucleons
in the Infinite Momentum Frame

A method for the analysis of interactions between fast deuterons and nucleons is developed taking into account both the relativistic effects in the deuteron and the mechanism of their interaction. The inclusive proton spectra and the polarisation characteristics are investigated on the example of the fragmentation type processes of deuterons on nucleons. A strong sensitivity of the deuteron polarisation tensor component T_{20} both to the reaction mechanism and to the relativistic structure of the deuteron is shown. The probable existence of the 6q-state in the deuteron in those reactions is discussed.

The investigation has been performed at the Laboratory of Nuclear Problems, JINR.

Preprint of the Joint Institute for Nuclear Research. Dubna 1989